International Journal of Scientific Research in Engineering and Management (IJSREM)
Volume: 06 Issue: 07 | July - 2022 Impact Factor: 7.185 ISSN: 2582-3930

SOLID STATE DIFFUSION OF SILVER NANOWIRESBY LARGE PLASTIC DEFORMATION

Ramya Ranjan Senapati,

Assistant Professor, Department of Mechanical Engineering,

Dhaneswar Rath Institute of Engineering & Management Studies, Odisha, India

Prakash Chandra Sha,

HOD, Department of Mechanical Engineering,

Divine Institute of Engineering and Technology, Odisha, India

ABSTRACT

The conventional cold welding concept was extended to nano scale, in which silver nanowires were welded together by large plastic deformation. A nano indenter was employed as a cold welding tool to visualize and conduct welding. The MD simulation shows that unlike single crystal nanowire, sufficient plastic deformation is key to realize successful welding when the two nano objects have large orientation mismatching. The lattice orientation of the joint interface is complex but no defects were found in both experimental and simulation.

SOLID STATE DIFFUSION OF SILVER NANOWIRES BY LARGE PLASTIC DEFORMATION

Since interconnect formation is critical for the assembly and integration of nano components to enable nano electronics- and nano systems related applications, nano joining is currently under intensive development. The nano joining methods include laser beam, electron beam, soldering, sintering, resistance welding, and ultrasonic welding. Most of these processes are designed to make thousands of joints simultaneously. However, few methods can join two targeted nano wires while leaving the surrounding nano objects intact, because nano scale-sized heat sources are hard to obtain. Cold welding does not require any heat source and as such becomes an attractive solution for bottom-up assembly at nano scale. In terms of the conventional cold welding method, pressure is used to producea weld at room temperature with substantial deformation at the weld. Obviously, macroscopic deformation is the key process factor because during deformation surface oxides are broken and more contact area is created between clean metallic surfaces inducing diffusion and re-crystallization at

the interface, and hence bonding. Therefore, whether this process concept could be extended to nano scale is determined by the plastic deformability of the nano objects. In this paper, the conventional cold welding concept was extended to nano scale, in which two targeted silver nanowires were welded together at room temperature and atmosphere environment by large plastic deformation, not by the agglomerative behavior of nano objects.

The silver nanowires were prepared in water in a seeded polyol solution with PVP as a structure directing reagent as previously described. Electron diffraction patterns confirmed that the nanowires were fivefold twinned with pentagonal cross section, and the axis was oriented along the b100N direction. TEM images showed that organic shells covering the surface of synthesizedAg nanowires had a 2.5–5 nm thickness. The Ag nanowires (NWs) solution was drop-cast onto a polished single crystal silicon sheet. A microhardness indenter was used to mark the location of the nanowires by conducting micro-indentations. The morphology of the nanowires used in these experiments was examined by Scanning Electron Microscopy (SEM), before and after cold welding. A Hysitron TriboIndenter nano indenter in conjunction with an AFM was used to perform imaging and cold welding tests. A three-sided pyramidal diamond (Berkovich) indenterwas selected to image and locate the nanowires and then in situ indent the wires with the same tip. The force–displacement curves were recorded with a resolution of 1 nN and 0.04nm, respectively. The nano joints were cross-sectioned using the Focused Ion Beam (FIB) (Zeiss NVision 40). A tungsten coating was deposited prior to FIB milling to protect the nanowire surfaces upon exposure to the Ga + beam.

Before cold welding tests, nanoindentation was performed on single nanowires in order to confirm if sufficient plastic deformation of the fivefold twinned pentagonal silver nanowires could occur before fracture. An array of indents with different loads was successfully conducted on one single silver nanowire (~400 nm in diameter and larger than 20 μm in length) for the purpose of comparison. and 1c show the indents on one single nanowire under the loads of 50 μN and 400 μN, respectively. Figs. 1b and 1d are the high magnification images of Figs.1a and 1c, respectively. Fig. 1e shows the load-depth curve under different indentation loads. The nanowire remained straight after the indentation tests and did not move, suggesting that the adhesion forces between the nanowire and the substrate were strong enough to prevent it from rolling or being dragged during the nanoindentation test and the scan after the test [14,15]. The shapes of the nanowire after indentation tests in Fig.1b (50 μN) and Fig. 1d (400 μN) indicated that a considerable amount of plastic deformation occurred. The 400 μN indented Ag nanowire was very flat and the maximum width was about twice the original diameter, whereas the 50 Mn indented nanowire was considerably thicker and narrower than that indented at 400 μN. Some grain boundaries are shown in Fig. 1d and the grain size was in the range of tens to few hundreds of nanometers. It suggests that new grains formed after large scale (more than 50%) plastic deformation.

When the maximum load was close to 50 μN (the inserted picture in Fig. 1e), the indentation depth was 24 nm which was 6% of the nanowire height. The hardness and elastic modulus values of the silvernanowire were measured to be about 0.63 and 45 GPa, respectively. The measured hardness of nanowire was higher than that of the bulk silver (about 0.4 GPa when indentation depth was larger than 1 μm), but smaller than nanowires with about 45 nm diameter (about 0.87 GPa when indentation depth was less than 15 nm) . An obvious pop-in mark was found in the curve of the
50 μN indentation load, which indicates plastic deformation associated with dislocation nucleation and motion [17–19]. A similar phenomenon was also observed in nanoindentation of silver nanowires (less than 100 nm in diameter) by both AFM and Berkovich nanoindenter tip.

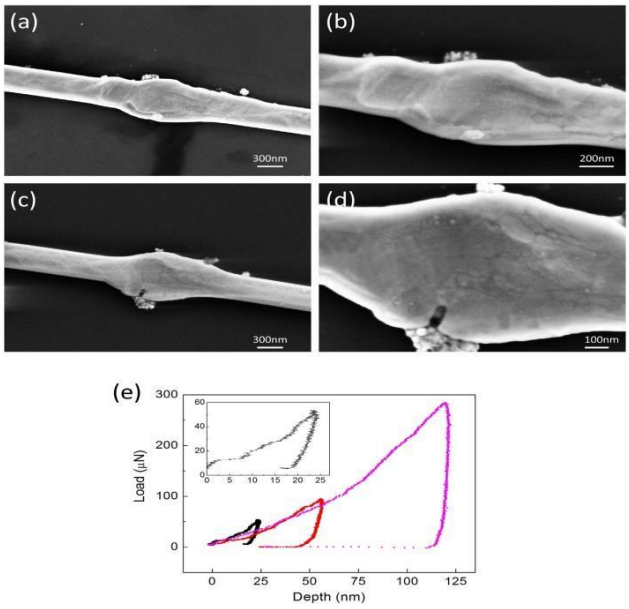

Fig. 1. Nano Indentations on single nanowire: (a) and (b) morphology of nanowire after 50 μN indentation load; (c) and (d) morphology of nanowire after 400 μN indentation load; (e) load-depth curve of different loads on the same nanowire, the insert is 50 μN. (For interpretation of the references to color in this figure, the reader is referred to the web version of this article.)

The AFMmode of the nanoindenter can visualize the nanowires and locate a specific indent zone, making the selective cold welding process possible, in which two crossed nanowires can be visualized and cold welded without affecting the surrounding nanowires. Fig. 2 shows the crossed silver nanowires after cold welding by nanoindenter. When the load was 50 μN (Fig. 2a), no significant plastic deformation was found in the wires and a barely observed indent appeared on the top wire (inserted picture in Fig. 2a). When the load was larger than 400 μN, the top wire had a large chance to fracture and Fig. 2b shows a typical result. When the load was between 200–300 μN, a sound weld could be conducted as shown in Fig. 2c. The joint showed obvious plastic deformation and the rest of the nanowires stayed in the original shape. When the load was between 300–400 μN, the crossed wires could still be welded but the joint showed that the top wire broke and attached to the bottom wire, as shown in Fig. 2d. Therefore, the process window of cold welding silver nanowires was 200–300 μN forNI with~400 nm in diameter.

Fig. 1. Nano Indentations on singlenanowire: (a) and (b) morphology of nanowire after 50 μN indentation load; (c) and (d) morphology of nanowire after 400 μN indentation load; (e) load-depth curve of different loads on the same nanowire, the insert is 50 μN. (For interpretation of the

references to color in this figure, the reader is referred to the web version of this article.)

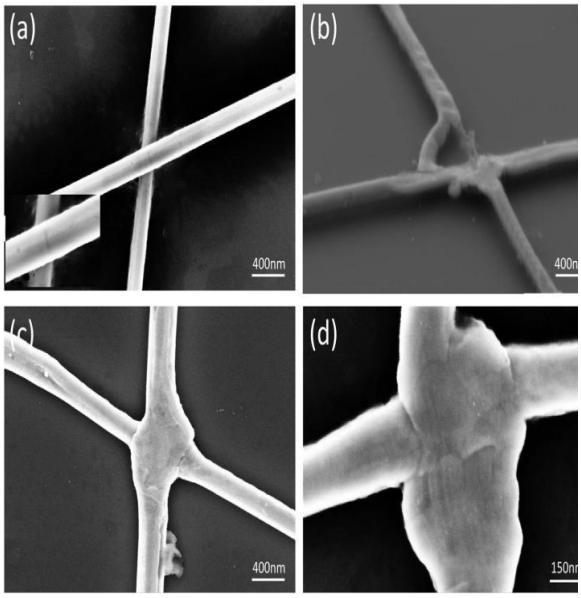

Fig. 2. Cold welding of silver nanowires under different loads: (a) 50 μN; (b) 400 μN; (c) 250 μN; (d) 300 μN. 400 μN, the top wire had a large chance to fracture and Fig. 2b shows a typical result. When the load was between 200– 300 μN, a sound weld could be conducted as shown in Fig. 2c. The joint

showed obvious plastic deformation and the rest of the nanowires stayed in the original shape. When the load was between 300–400 μN, the crossed wires could still be welded but the joint showed that the top wire broke and attached to the bottom wire, as shown in Fig. 2d. Therefore, the process window of cold welding silver nanowires was 200–300 μN forNI with~400 nm in diameter.

In order to examine the joint interface of the coldwelded nanowires, FIB was used to cut cross section samples, as shown in Fig. 3. The same nanowires before and after cold welding are shown in Figs. 3a and 3b, respectively. The white dotted line in Fig. 3b indicates the cross section direction cut by FIB. Figs. 3c and 3d show different cross sections during FIB cutting. The nanowires were covered with a tungsten coating on the top to avoid ion beam damage and the dark surface beneath the nanowires was the polished single crystal silicon substrate. In Figs. 3c and 3d, it is shown that the weld interface revealed no defects in different cross sections, indicating that a relatively large welded area was obtained. Fig. 3e is the high magnification image of Fig. 3c. Fig. 3f is the load depth curve of this joint. The loadwas around 270 μNwhichwas similar to the pink curve in Fig. 1e.

The simulations were conducted by using LAMMPS and the detailed configuration of the simulation can be found elsewhere. For comparison purposes both pentagonal and single crystal nanowires were simulated by moving a spherical virtual indenter at a constant velocity of 2 m/s. Fig. 4a shows the load–depth curves and the bottom snapshots are atomistic configurations of single nanowires at different stages of deformation. It can be observed that at the early stage of the indentation, the single crystal (SC) nanowire and the five-twined nanowire (FT) perform very similar load–displacement curve regardless of the different microstructures. When the indentation depth further increases to above 10 Å, the load of SC nanowire becomes lower than that of FT nanowire. In the SC nanowire, the atomic configuration shows that the appearance of hcp atoms in fcc nanowire presents stacking faults left after activities of Shockley partial dislocations. With an increasing strain, more partial dislocations initiate in the planes and interact with each other due to the absence of a strong obstacle to their propagation. When twin boundaries exist and are

perpendicular to the stress as shown in FT nanowire, fivefold coherent twin boundaries provide a strong internal barrier to dislocation motion. The simulation shows that those dislocations in FT nanowire reach the twin boundaries and become immobilized and accumulated at the twin boundaries, making the newly nucleated dislocations unable to escape freely and resulting in significant strain hardening.

Fig. 4b shows the load–displacement curves of the cold welding process by indentingtwo cross placed nanowires. The snapshots at bottom are at different stages of the cold welding process. The simulation shows that the SC and FT nanowires have similar load–displacement curves but different joint formation processes and interfacial configurations. The load–displacement curve shows that both SC and FT contain large slip steps and discrete strain bursts, suggesting that plastic deformation occurs. The snapshots of SC nanowire indicate that at an early stage of deformation the two nanowires have "oriented–attached", and theatoms at the interface are perfectly aligned. As the indentation depth increases, more dislocations and stacking faults appear and the joined area also increases. This is very similar to the results by Lu et al. (experiment) and Pereira et al. (MD simulation), in which they believed that matching orientation is critical to realizing sound welding.

However, the snapshots of cold welding of FT nanowires show a different process with SC nanowires. At the early stage of deformation, the two FT nanowires are attached, but the atomic configuration at the interface has large mismatch and high interfacial energy, and the joined area is also small compared to that of SC nanowire. It demonstrates that sound and reliable cold welding of FT nanowire are hard to occur by mechanical contact alone or under relatively low applied pressures due to the orientation mismatching. As the indentation depth increases, the joined area increases and the interfacial configuration becomes complex, containing large angle grain boundaries, well aligned atoms, and stacking faults. Most of the deformation occurs in the upper FT nanowire, and the bottom FT nanowire (especially the bottom three twins) has very little deformation due to the pronounced strain hardening effect by the coherent twin boundaries. This is also evidenced by the joint formation in Fig. 2, in which the upper FT nanowire had obviously larger deformation than that of the bottom nanowire.

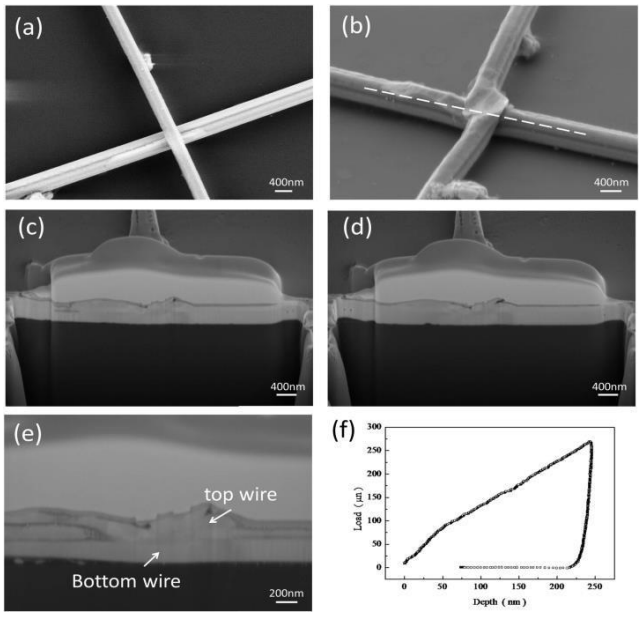

Fig. 3. Microstructure of the coldwelded crossed nanowires: (a) before welding; (b) after welding; (c) cross section by FIB; (d) further cut by FIB; (e) high

magnification image of the joint interface; (f) load-depth curve of this joint.

The bottom-up synthesized nanowires were normally covered by organic shells,which was to control the growth direction and to prevent agglomeration of nanowires. Therefore, the two crossed placed nanowires would not weld together by contact only,even if their orientations were perfectly matched. During the cold welding process, large plastic deformation occurred which induced the breaking of the organic shells and surface oxide layers. Cleaner and larger contact areas appeared on the faying surfaces as more plastic deformation occurred. This is another advantage of this nano coldwelding technology which can be operated in a normal atmosphere environment and has no strict requirements on the surface quality. the conventional cold welding concept was extended to nanoscale, in which two targeted silver nanowires were welded together by large plastic deformationwithout affecting the surrounding nano objects. A nanoindenter was used as a cold welding tool and conducted at room temperature and normal atmosphere environment, making the process easier and low cost. The MD simulation shows that unlike single crystal nanowire, the cold welding of five twined nanowire cannot occur spontaneously by contact alone due to the orientation mismatching. Sufficientplastic deformation is key to realize successful welding when the nano objects have large orientation mismatching. The lattice orientation of the joint interface is complex but no defects were found in both experimental and simulation.

Acknowledgments

This work was supported by National Natural Science Foundation of China (Grant No. 51375261 51405258), by The Natural Science Foundation of Beijing (Grant No. 3132020), by The Specialized Research Fund for Doctoral Program Of Higher Education (Grant No.20130002110009), by the National Sciences and Engineering Research Council (NSERC) of Canada, and by Tsinghua University Initiative Scientific Research Program (Grant No.2010THZ 02-1 2013Z02-1). The authors would like to thankMr. Fred Pearson from the Canadian Center for ElectronMicroscopy, McMaster University, for help with TEM. Appreciation is also expressed to Prof. Scott Lawson for useful discussions.

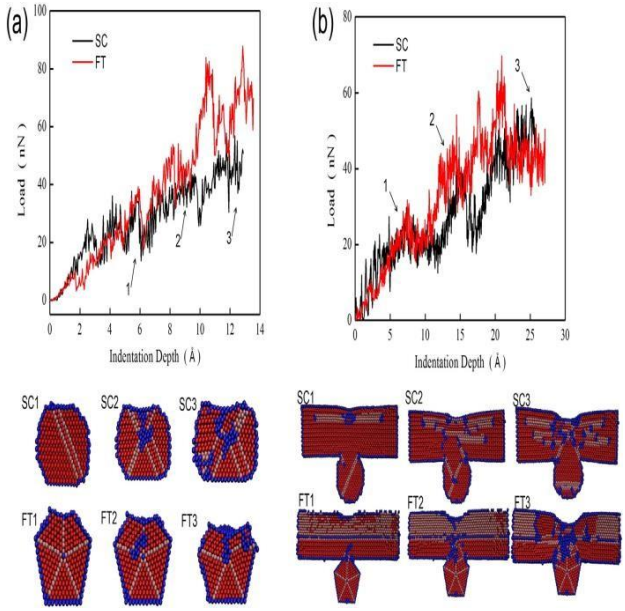

Fig. 4. Load–displacement curves of single crystal (SC) and five-twined (FT) nanowires: (a) single nanowire indentation; (b) cold welding of two crossed nanowires.

Snapshots at different stages of deformation are shown fromSC1–SC3 (for SC nanowire) and FT1–FT3 (for FT nanowire), respectively. The atoms are colored by: red fcc, pink hcp; blue other. (For interpretation of the references to color in this figure legend, the reader is referred to the web version of this article.)

References

[1] Q. Cui, F. Gao, S. Mukherjee, Z. Gu, Small 5 (2009) 1246–1257.

[2] S.J. Kim, D.-J. Jang, Appl. Phys. Lett. 86 (2005) 033112.

[3] L. Liu, P. Peng, A. Hu, G. Zou, W. Duley, Y.N. Zhou, Appl. Phys. Lett. 102 (2013)073107.

[4] I. Jang, S.B. Sinnott, D. Danailov, P. Keblinski, Nano Lett. 4 (2004) 109–114.

[5] L. Liu, H. Huang, A. Hu, G. Zou, L. Quintino, Y. Zhou, Nano-Micro Lett. 5 (2013).

[6] E. Ide, S. Angata, A. Hirose, K.F. Kobayashi, Acta Mater. 53 (2005) 2385–2393.

[7] H. Tohmyoh, T. Imaizumi, H. Hayashi, M. Saka, Scr. Mater. 57 (2007) 953–956.

[8] B. Zhao, B. Yadian, D. Chen, D. Xu, Y. Zhang, Appl. Surf. Sci. 255 (2008) 2087–2090.

[9] C. Chen, L. Yan, E.S.-W. Kong, Y. Zhang, Nanotechnology 17 (2006) 2192.

[10] Y. Lu, J.Y. Huang, C. Wang, S. Sun, J. Lou, Nat. Nanotechnol. 5 (2010) 218–224.

[11] S. Garroni, S. Enzo, F. Delogu, Scr. Mater. 83 (2014) 49–52.

[12] S. Garroni, S. Soru, S. Enzo, F. Delogu, Scr. Mater. 88 (2014) 9–12.

[13] P. Peng, L. Liu, A.P. Gerlich, A. Hu, Y.N. Zhou, Part. Part. Syst. Charact. 30 (2013) 420–426.

[14] X. Li, H. Gao, C.J. Murphy, K. Caswell, Nano Lett. 3 (2003) 1495–1498.

[15] M. Lucas, A.M. Leach, M.T. McDowell, S.E. Hunyadi, K. Gall, C.J. Murphy, E. Riedo, Phys. Rev. B 77 (2008) 245420.

[16] M. Zhao, W.S. Slaughter, M. Li, S.X. Mao, Acta Mater. 51 (2003) 4461–4469.

[17] D. Christopher, R. Smith, A. Richter, Nanotechnology 12 (2001) 372.

[18] S. Buzzi, M. Dietiker, K. Kunze, R. Spolenak, J. Löffler, Philos. Mag. 89 (2009) 869–884.

[19] Q. Yu, Z.-W. Shan, J. Li, X. Huang, L. Xiao, J. Sun, E. Ma, Nature 463 (2010) 335– 338.

[20] S. Plimpton, J. Comput. Phys. 117 (1995) 1–19.

[21] M. Sun, R. Cao, F. Xiao, C. Deng, Comput. Mater. Sci. 79 (2013) 289–295.

[22] K.A. Afanasyev, F. Sansoz, Nano Lett. 7 (2007) 2056–2062.

[23] T. Filleter, S. Ryu, K. Kang, J. Yin, R.A. Bernal, K. Sohn, S. Li, J. Huang, W. Cai, H.D. Espinosa, Small 8 (2012) 2986–2993.